PHYSICAL REVIEW C **69**, 011301(R) (2004)

Rotation-driven spherical-to-deformed shape transition in $A \approx 100$ nuclei and the cranked interacting boson model

Pavel Cejnar[1,2,*] and Jan Jolie[2,†]
[1]*Institute of Particle and Nuclear Physics, Charles University, V Holešovičkách 2, 180 00 Prague, Czech Republic*
[2]*Institute of Nuclear Physics, University of Cologne, Zülpicherstrasse 77, D-50937 Cologne, Germany*
(Received 12 November 2003; published 28 January 2004)

Using the cranked interacting boson model, we estimate critical frequencies for the rotation-induced spherical-to-deformed shape transition in $A \approx 100$ nuclei. The predictions are shown to roughly agree with the backbending frequencies deduced from experimental yrast sequences in these nuclei.

DOI: 10.1103/PhysRevC.69.011301 PACS number(s): 21.10.Re, 21.60.Ev, 27.60.+j

It is now well documented that the nuclear ground-state shapes exhibit sudden changes with varying nucleon numbers—changes that are described in close analogy with thermodynamic phase transitions (see, e.g., Refs. [1–13]). In particular, signatures of transitions between spherical and various deformed shapes (prolate or oblate axisymmetric ellipsoids) clearly follow from spectroscopic data characterizing some chains of nuclei [1,3,7,9,11,13]. Real nuclei thus seem to sample—depending on underlying energies and occupancy of the single-particle orbitals—the phase diagram of the quadrupole geometric model or, equivalently, of the interacting boson model (IBM).

Another kind of a structural "phase transition," the one that concerns individual nuclides rather than isotopic/isotonic sequences of nuclei, manifests itself as the well-known backbending effect [14,15]. Observed in many yrast-band sequences, this phenomenon is usually interpreted as a crossing of two rotational bands with different deformations, pairing properties, and/or angular-momentum alignments along the rotational axis [16–18]. The yrast state thus flips between the corresponding configurations (with different values of the moment of inertia), which can be seen as a rotation-driven quantum phase transition, similar to phase transitions of the ground-state shape. However, as recently pointed out by Regan *et al.* [19], the picture involving the crossover between two rotational deformed bands may be misleading if applied to nuclei with vibrational-like ground-state properties. For these nuclei, a change from spherical (vibrational) to deformed (rotational) structure was proposed as an alternative explanation of the observed backbending behavior. Indeed, making use of the γ-ray energy over spin (E-GOS) plots, the cited authors claim that the yrast-band sequences in a number of vibrational Cd, Pd, and Ru nuclei exhibit a signature of the spherical-to-deformed evolution at spins of about 10 or 12 $\hbar$.

Microscopically, the evolution is caused by several effects related to the fermionic degrees of freedom. Notably, both collective two-particle–two-hole excitations leading to more deformed intruder states with a characteristic energy dependence on the number of valence nucleons [20] as well as noncollective Coriolis-driven pair breaking leading to alignment [21] have to be involved. The latter mechanism can also be consistently described within the cranked shell model, applicable around mass 100, based on the alignment of a $(h_{11/2})^2$ neutron pair coupled to spin $10\hbar$ [22].

The purpose of this Rapid Communication is to interpret experimental results given in Ref. [19] from new theoretical perspective [23] using the Landau theory of phase transitions in the framework of the cranked IBM. In the cranking extension, the IBM is handled as a semiclassical model (the total number of bosons $N \to \infty$) to determine Bohr variables β and γ as a function of the rotational frequency ω and Hamiltonian parameters (η and χ coordinates in the extended Casten triangle [10]). Various phases are located in distinct regions of the parameter space $\omega \times \eta \times \chi$ [23,24].

While earlier attempts to apply the Landau theory to rotating (hot) nuclei [25] implied that the rotation did not induce a crossover between spherical and deformed shapes (since the deformation evolves smoothly with the onset of cranking), the cranking in the IBM case leads to the conclusion that the rotation-induced spherical-to-deformed phase transition is theoretically possible with a more general ansatz for quadrupole geometric variables employed in the calculation. The dependence of nuclear deformation on the rotational frequency, as determined in Refs. [23,24], closely resembles the abrupt quenching of superconductivity under increasing magnetic field. In this analogy, the superconducting and normal phases correspond to the spherical ($\beta = 0$) and deformed ($\beta \neq 0$) shapes, respectively, while ω plays the role of the field strength. At a certain critical frequency ω_c the shape flips from spherical to deformed, similarly as the paired superconducting phase breaks into a normal phase at a critical field. Due to the analogy of the backbending phenomenon with the behavior of superconductors, the idea of a pairing transition [16] has been invoked in high-spin physics. In view of the new result [23], however, it turns out that the same behavior can be associated with a shape transition, as well, which supports the viewpoint proposed in Ref. [19].

To compare experimental data on the yrast-band shape transition in vibrational nuclei with predictions of the cranked IBM, one may try to determine from the theory the critical angular momentum for which the spherical yrast state transforms into a deformed one. This angular momentum is, in principle, available from experimental data, using for ex-

*Electronic address: pavel.cejnar@mff.cuni.cz
†Electronic address: jolie@ikp.uni-koeln.de

TABLE I. Comparison of experimental and theoretical values of the critical rotational frequency, the latter obtained from the cranked IBM with η fitted to low-spin yrast energies ($\Delta E_{\rm rms}$ measures the quality of the fit).

Nucleus	$\omega_c^{\rm ex}$ (MeV/$\hbar$)	$\omega_c^{\rm th}$ (MeV/$\hbar$)	η	$\Delta E_{\rm rms}$ (keV)
^{108}Cd	0.40(17)	0.37	0.94	177
^{110}Cd	0.32(15)	0.38	0.97	168
^{112}Cd	0.38(2)	0.31	0.93	36
^{114}Cd	0.30(6)	0.32	0.99	74
^{104}Pd	0.35(5)	0.33	0.94	132
^{106}Pd	0.36(8)	0.33	0.97	130
^{108}Pd	0.33(6)	0.23	0.89	93
^{100}Ru	0.45(5)	0.14	0.82	83
^{102}Ru	0.36(5)	0.24	0.88	91
^{100}Mo	0.37(2)	0.22	0.87	49

ample the E-GOS plots [19]. However, since the IBM spherical phase is formed by a condensate of only *s* bosons, it carries zero angular momentum for any ω up to ω_c. One thus has to extract from yrast data not the critical spin but rather the critical frequency. This is indeed possible with the aid of the backbending diagram, where the yrast spin $I \approx \sqrt{I(I+1)}$ (or a related quantity) is plotted against $E_I^\gamma/2 = (E_{I+1} - E_{I-1})/2$, with E_I denoting the yrast-state energy for spin I, thus $E_I^\gamma/2 = \partial E_I/\partial I \approx \omega_I$ approximating the rotational frequency at angular momentum I. The well-known *S*-shaped structure in backbending plots which would (in the rotational picture) be interpreted as a change of the moment of inertia, is correlated with the evolution from hyperbolic to roughly constant behavior in the corresponding E-GOS plots, as observed in vibrational nuclei [19]. Therefore, it can be used to estimate the critical frequency ω_c.

Experimental values of the critical frequency, as extracted from the data [19,26–28,30] for a subset of nuclei studied in Ref. [19], are given in Table I. The mean value ($\omega_c^{\rm ex}$) and its error (in parentheses) were obtained as the central point and the width, respectively, of the *S*-shaped structure in the backbending plot corresponding to the given nucleus. Let us stress that this method does not imply the insistence on the rotational interpretation of the backbending effect in vibrational nuclei: in the present picture, the yrast sequence above ω_c is assumed to be rotational, while the spectrum below ω_c rather corresponds to an anharmonic vibrator.

To analyze experimental data in the $A \approx 100$ region, we use the well-known IBM Hamiltonian

$$H = \hbar\Omega\left[\eta n_{\rm d} - \frac{1-\eta}{N} Q \cdot Q\right] \qquad (1)$$

where N is the total number of bosons, $n_{\rm d}$ the *d*-boson number operator, and $Q = (d^\dagger \tilde{s} + s^\dagger \tilde{d})^{(2)} + \chi(d^\dagger \tilde{d})^{(2)}$ the quadrupole operator. It is clear that this Hamiltonian is too simple to fully describe complete spectra of real even-even nuclei, but, at the same time, it is known to capture some essential features of basic collective states in these nuclei [11,13]. H in Eq. (1) has in principle three control parameters: (i) the quadrupole parameter χ, taking values from the interval $[-\sqrt{7}/2, +\sqrt{7}/2]$ as the deformed shape evolves from a prolate to oblate form; we set $\chi = 0$ for the $A \approx 100$ nuclei studied here (implying that we stay at or close to the γ-soft transitional line of the Casten triangle), (ii) $\eta \in [0, 1]$ governing the evolution between the deformed, O(6) in case of $\chi = 0$, and spherical, U(5), ground state, and (iii) the overall scaling frequency $\Omega > 0$. The phase transition from a deformed to spherical ground-state shape appears as η crosses $\eta_c = 0.8$. Thus the nuclei with potential to host the spherical-to-deformed transition along their yrast line must be located close to the U(5) vertex—within the interval $\eta \in [0.8, 1]$.

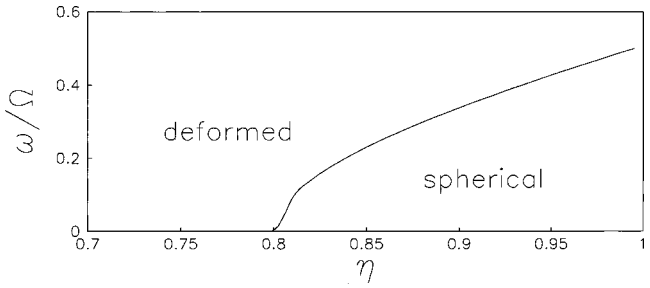

FIG. 1. Cranking phase diagram of Hamiltonian (1).

The values of η and Ω in Eq. (1) were fitted to experimental yrast energies below the critical spin in the nuclei studied, namely to yrast states up to $I = 10\hbar$ in Cd isotopes and $I = 12\hbar$ in Pd, Ru, and Mo. The resulting values of η are given in Table I. The rms deviation of level energies, $\Delta E_{\rm rms} = \sqrt{\Sigma_I \Delta E_I^2/n}$ (with n standing for the number of fitted levels and ΔE_I for the difference between experimental and theoretical energies for the yrast state with a given I), measures the quality of the fit.

Properties of the Hamiltonian (1) in the rotating frame were analyzed in Refs. [23,24] yielding the deformation parameters β and γ as a function of dimensionless cranking frequency $\tilde{\omega} = \omega/\Omega$. Note that the deformation parameters in the cranked IBM are not directly connected with the coherent-state coefficients, as in the standard IBM geometric analysis [1], but follow from an analogous parameterization of the average quadrupole-moment components, i.e., from $\langle Q_0 \rangle = \beta \cos\gamma$ and $\sqrt{2}\langle Q_2 \rangle = \beta \sin\gamma$. The dependence of deformation parameters on η and ω, as it follows from the IBM cranking calculations, can be found in Figs. 3 and 5 of Ref. [24]. The critical cranking frequency is an increasing function of $\eta \in [0.8, 1]$ with $\tilde{\omega}_c = 0$ at $\eta \leqslant 0.8$ and $\tilde{\omega}_c = 0.5$ at $\eta = 1$, see Fig. 1. By fitting the values of η and Ω, as explained above, we are therefore able to determine the absolute theoretical value $\omega_c^{\rm th} = \tilde{\omega}_c(\eta)\Omega$. In Table I, this quantity is compared with experimental critical frequencies in the nuclei studied.

Before discussing the degree of agreement between theoretical and experimental values in Table I, we should point out that not all nuclei considered in Ref. [19] are listed here. The fits of experimental yrast energies in Mo isotopes with

$A \geqslant 102$ and in Ru with $A \geqslant 106$ place these nuclei well to the deformed side of the Casten triangle, implying $\omega_c^{th}=0$. This is in accord with mostly rotational character of the corresponding E-GOS plots [19]. The ^{102}Mo, ^{104}Ru, and also ^{110,112}Pd nuclei seem to be very close to the separatrix between spherical and deformed shapes. Although the E-GOS plots in these nuclei still show behaviors characteristic for the spherical ground-state configuration, our fit gives values of η already near to η_c, implying ω_c zero or negligible (namely, we get $\eta=0.81$ for ^{110,112}Pd, $\eta=0.80$ for ^{104}Ru, and $\eta=0.68$ for ^{102}Mo). For ^{104}Ru, the latter result in fact agrees with Ref. [31], where this nucleus was proposed as a candidate for the E(5) critical-point symmetry. Finally, we did not analyze ^{98}Mo because of the lack of data, and ^{104,106}Cd and ^{102}Pd, where IBM only gives yrast states up to $I=8$ or $10\,\hbar$ (since $N=4$ or 5).

The theoretical and experimental critical frequencies listed in Table I show very good agreement for the nuclei placed close to the U(5) vertex, i.e., for those with $\eta>0.9$. However, as the fitted η approaches 0.8, the predicted critical frequency decreases and deviates from the experimental value. An extreme example is ^{100}Ru, which is located indeed too close to η_c in our fit and thus exhibits rather small value of ω_c^{th}. This cannot be improved by allowing for nonzero values of χ. Let us note that qualitatively the same trend as in the cranked IBM would be generally expected in the microscopic picture, since the intruder orbitals lower in energy as the midshell is approached. The presently analyzed data, however, seem to exhibit rather a constant value of the critical frequency and then a sudden change to $\omega_c^{ex}=0$. This behavior should be checked in other relevant regions of the nuclear chart. On the other hand, we see that in spite of apparent simplifications involved in our approach it is possible to correctly reproduce the critical frequencies in truly vibrational nuclei and to roughly predict the border of the vibrational-like region in the given part of the nuclear chart. Let us note that on the microscopic level, the delayed backbend observed in ^{100}Ru seems to be connected with a suppressed population of the $(h_{11/2})^2$ neutron configuration, which is linked to the backbending plots in the given mass region [19,22].

We are aware that the weakest point of the present analysis is the oversimplified form of the Hamiltonian (1) in confrontation with experimental spectra, for instance the absence of an anharmonic term in the U(5) limit. This may in some cases lead to unphysical fits of η and thus to incorrect estimates of ω_c^{th}. To use the Hamiltonian (1) was necessary to keep a link with the analysis of Ref. [23]. The form (1) is common in studies of nuclear shape phases [5,8,10–13] and the extension into the cranking framework led to a particularly simple and clear perspective on the rotation-induced shape transitions. Nevertheless, similar analyses can in principle be done for other, more sophisticated nuclear collective Hamiltonians, even beyond the IBM scheme. The crucial observation is that with the generalized Landau theory of shape phase transitions in rotating nuclei (specifically, using general non-Hermitian coherent-state coefficients yielding a Hermitian physical quadrupole tensor [23]) one can obtain results that overcome previous analyses [25] just in the direction required by the new interpretation of experimental data [19].

Let us finally note that the approach proposed here differs substantially from that of Ref. [32] (recently reconsidered in Ref. [33]) where the backbending phenomenon in vibrational nuclei was interpreted using the IBM Hamiltonian in the exact U(5) limit with a negative coefficient at the second-order U(5) invariant. In this case, one indeed observes the yrast-band transition between $n_d=I/2$ and $n_d=N$ configurations (having, in this sense, different "deformations"), but the divergence of solutions for $N\rightarrow\infty$ makes it impossible to use the model in the classical limit (to speak in this context about a $\beta\rightarrow\infty$ "phase transition," as in Ref. [33], is thus very misleading). The cranking approach, in contrast, results in a picture where the yrast-band structural transition is indeed between spherical and deformed shapes and remains physical in the classical limit.

The authors thank R. F. Casten for valuable comments on the manuscript. This work was supported by the DFG and GAČR under Grant Nos. 436 TSE 17/6/03 and 202/02/0939, respectively. P.C. also thanks the University of Cologne for hospitality.

[1] A. E. L. Dieperink, O. Scholten, and F. Iachello, Phys. Rev. Lett. **44**, 1747 (1980); A. E. L. Dieperink and O. Scholten, Nucl. Phys. **A346**, 125 (1980).
[2] D. H. Feng, R. Gilmore, and S. R. Deans, Phys. Rev. C **23**, 1254 (1981).
[3] R. F. Casten, N. V. Zamfir, and D. S. Brenner, Phys. Rev. Lett. **71**, 227 (1993); R. F. Casten, D. Kusnezov, and N. V. Zamfir, *ibid.* **82**, 5000 (1999).
[4] E. López-Moreno and O. Castaños, Phys. Rev. C **54**, 2374 (1996).
[5] P. Cejnar and J. Jolie, Phys. Rev. E **61**, 6237 (2000).
[6] F. Iachello, Phys. Rev. Lett. **85**, 3580 (2000); **87**, 052502 (2001).
[7] R. F. Casten and N. V. Zamfir, Phys. Rev. Lett. **85**, 3584 (2000); **87**, 052503 (2001).
[8] P. Cejnar, V. Zelevinsky, and V. V. Sokolov, Phys. Rev. E **63**, 036127 (2001).
[9] J. E. García-Ramos, C. De Coster, R. Fossion, and K. Heyde, Nucl. Phys. **A688**, 735 (2001).
[10] J. Jolie, R. F. Casten, P. von Brentano, and V. Werner, Phys. Rev. Lett. **87**, 162501 (2001).
[11] J. Jolie and A. Linnemann, Phys. Rev. C **68**, 031301(R) (2003).
[12] P. Cejnar, S. Heinze, and J. Jolie, Phys. Rev. C **68**, 034326 (2003).
[13] E. A. McCutchan *et al.* (unpublished).
[14] A. Johnson, H. Ryde, and J. Sztarkier, Phys. Lett. **34B**, 605 (1971).
[15] H. Morinaga and T. Yamazaki, *In-Beam Gamma-Ray Spectroscopy* (North-Holland, Amsterdam, 1976).

[16] B. R. Mottelson and J. G. Valatin, Phys. Rev. Lett. **5**, 511 (1960).
[17] S. Åberg, H. Flocard, and W. Nazarewicz, Annu. Rev. Nucl. Part. Sci. **40**, 439 (1990).
[18] S. G. Nilsson and I. Ragnarsson, *Shapes and Shells in Nuclear Structure* (Cambridge University Press, Cambridge, UK, 1995).
[19] P. H. Regan *et al.*, Phys. Rev. Lett. **90**, 152502 (2003).
[20] K. L. G. Heyde, J. Jolie, J. Moreau, J. Ryckebush, M. Waroquier, P. Van Duppen, M. Huyse, and J. L. Wood, Nucl. Phys. **A466**, 189 (1987).
[21] F. S. Stephens and R. S. Simon, Nucl. Phys. **A183**, 257 (1972).
[22] P. H. Regan *et al.*, J. Phys. G **19**, L157 (1993); P. H. Regan, A. E. Stuchbery, and S. S. Anderssen, Nucl. Phys. **A591**, 533 (1995); P. H. Regan *et al.*, Phys. Rev. C **55**, 2305 (1997); **68**, 044313 (2003).
[23] P. Cejnar, Phys. Rev. Lett. **90**, 112501 (2003).
[24] P. Cejnar, Phys. Rev. C **65**. 044312 (2002).
[25] Y. Alhassid, S. Levit, and J. Zingman, Phys. Rev. Lett. **57**, 539 (1986); Y. Alhassid, J. Zingman, and S. Levit, Nucl. Phys. **A469**, 205 (1987).
[26] J. Blachot, Nucl. Data Sheets **91**, 135 (2000); **97**, 593 (2002); **64**, 1 (1991).
[27] D. De Frenne and E. Jacobs, Nucl. Data Sheets **89**, 481 (2000); **79**, 639 (1996); **72**, 1 (1994).
[28] B. Singh, Nucl. Data Sheets **81**, 1 (1997).
[29] A. O. Macchiavelli *et al.*, Phys. Rev. C **38**, 1088 (1988).
[30] M. Houry *et al.*, Eur. Phys. J. A **6**, 43 (1999); R. Krücken *et al.*, *ibid.* **10**, 151 (2001).
[31] A. Frank, C. A. Alonso, and J. M. Arias, Phys. Rev. C **65**, 014301 (2001).
[32] G. L. Long, Phys. Rev. C **55**, 3163 (1997).
[33] J. Shu, Y. Ran, T. Ji, and Y. X. Liu, Phys. Rev. C **67**, 044304 (2003).